AD-A057 081 WASHINGTON STATE UNIV PULLMAN DEPT OF CHEMISTRY F/G 7/4
CHEMICAL MEASUREMENTS IN THE PICOSECOND AND SHORTER TIME RANGE.(U)
MAR 78 S C PYKE , M W WINDSOR N00014-75-C-0535
UNCLASSIFIED TR-13-ONR NL

2 OF 2
AD
A057081

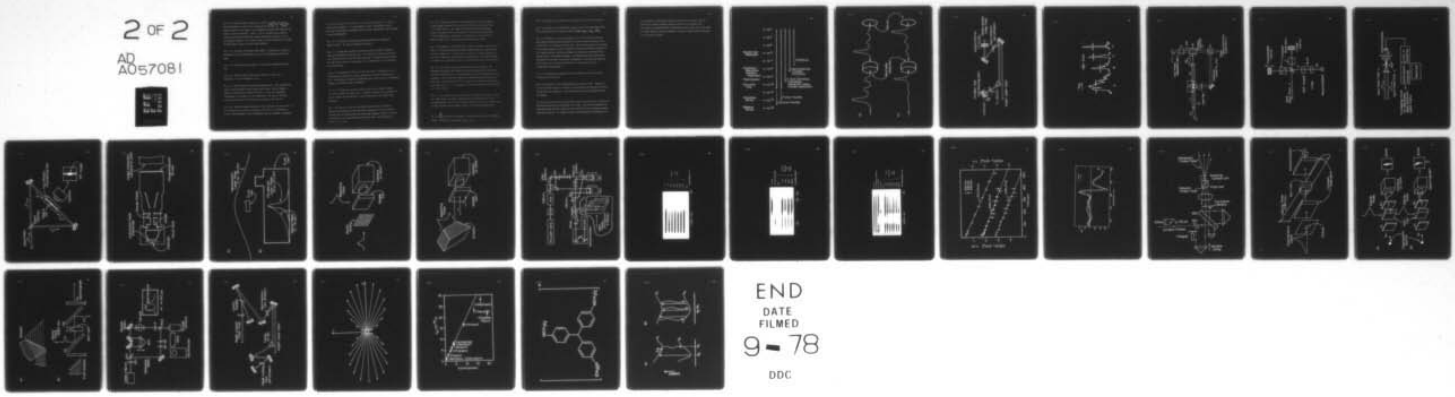

END
DATE
FILMED
9-78
DDC

Fig. 2.1.6 Ippen and Shank's adaptation of Weber's technique for pulse-width measurements of pulses from a modelocked CW dye laser (Laser Focus, July, 1977). Second harmonic output is at an angle to the fundamental frequency and eliminates the need for filters to separate ν from 2ν. One of the input pulse trains is chopped, and the lock-in amplifier provides synchronous detection of 2ν at the chopping frequency. This increases signal to noise dramatically, and weak (second harmonic) signals are more easily measured.

Fig. 2.1.7 Two photon fluorescence (TPF) method. Pulsewidths are generally determined from a microdensitometer trace of the photographed fluorescence image.

Fig. 2.1.8 Streak tube from an Imacon II streak camera (Hadland Photonics, Ltd.)

Fig. 2.3.1 Spatial extent of laser pulses relative to same size: A) pulsewidth = 1 ns; B) pulsewidth = 10 ps.

Fig. 2.3.2 Malley-Rentzepis crossed beam technique (51). The interrogating pulse is passed through a Ronchi ruling, about a meter from the ruling, to smooth its cross-sectional intensity profile. In this way homogeneous illumination of the sample cell is accomplished. This assures reasonably accurate determination of decay kinetics from optical wake profiles.

Fig. 2.3.3 Echelon technique developed by Topp, Rentzepis, and Jones (52). If the bleaching pulse uniformly illuminates the sample, a microdensitometer trace of the photograph of the interrogating pulse will resemble a histogram

(of intensity bands) reflecting decay of excited state absorbance or return of ground state absorbance. If a spectrograph is used, a photographic record will also include spectral information and allow the calculation of rate constants at several wavelengths.

Fig. 2.3.4 Picosecond flash photolysis apparatus developed by Magde and Windsor (55,56). See text for detailed description.

Fig. 2.3.5 Photographic record of excited state decay of BDN in iodoethane using the Magde-Windsor technique (56). The film plate is moved and the delay time between excitation pulse and monitoring pulse is changed between exposures. The dark central portion of each image is due to absorbance of the continuum by the excited state.

Fig. 2.3.6 Photographic record of excited state decay of $[(OEP)SnCl_2]$ in 1,2-dichloroethane showing both S_1 and T_1 absorption as studied by Magde et al., (57). The persistent excited state absorbance due to the T_1 state is particularly evident in the 500 and 2,000 ps exposures.

Fig. 2.3.7 Photographic record of excited state decay of DODCI in ethanol as studied by Magde and Windsor (55). Bleaching of ground state absorbance can be seen between 560 and 590 nm as a light central band in the shorter-time exposures.

Fig. 2.3.8 Kinetics of one of the electron transfer steps in bacterial photosynthesis measured at three different wavelengths in reaction centers isolated from the photosynthetic bacterium, Rps. viridis. Figure 2.3.9 shows the spectra of the states before and after this step. From the paper by Holten et al., (196).

Fig. 2.3.9 Absorbance changes at room temperature for reaction centers of Rps. viridis, measured after time delays of 20 ps (open circles) and 1 ns (closed circles). The change in the difference spectrum between the two time delays reflects the transfer of an electron from a molecule of bacteriopheophytin to ubiquinone. The kinetics of this process are shown in Figure 2.3.8. From the paper by Holten et al., (196).

Fig. 2.3.10 Schematic of the method used to measure transient kinetics by the decay of a grating (interference pattern) produced when two coherent pulses cross in a sample cell. The interference pattern is a spatial modulation in the ratio of ground to excited states and persists with a lifetime dependent on excited state relaxation or decay of induced orientational anisotropy (64).

Fig. 2.4.1 Kerr shutter used in measuring fluorescence lifetimes. The photomultiplier detects the signal that passes through the Kerr cell coincident with the gating pulse. By delaying the arrival of the gating pulse, the intensity of the fluorescence signal can be measured and plotted versus the delay time. The resolution of the Kerr shutter is a function of the width of the gating pulse ($\sim$ 5 ps). Consequently, this method works best when lifetimes are $\gtrsim$ 50 ps (69,70).

Fig. 2.4.2 Kerr shutter used to measure short fluorescence lifetimes ($\lesssim$ 50 ps) in a single pulse: A) Kinetic data are obtained from OMA output of from a microdensitometer trace of the photographic image; B) Kinetic and spectral data are both available in this design P_1 and P_2 are crossed polarizers (72).

Fig. 2.4.3 B) A Kerr shutter incorporating a colinear gating pulse and fluorescence signal: A) Detail of transmitting echelon. (55).

Fig. 2.4.4 Streak camera technique for measurement of fluorescence lifetimes.

Fig. 2.5.1 Folded cavity configuration characteristic of the modelocked CW dye laser systems developed by Ippen and Shank (Laser Focus, July, 1977).

Fig. 3.1.1 Envelope of vectors reflecting the $\cos^2\theta$ distribution of ground state moments remaining after absorption of a pulse linearly polarized in the Y direction (θ is the angle off the X axis). The excitation pulse is travelling into the page along the z-axis. Molecules with transition moments perpendicular to Y remain unexcited, whereas the ensemble of molecules with moments nearly parallel with Y is maximally disturbed. The induced anisotropic distribution of moments will influence the relative transmission of the polarized light and will persist with a lifetime characteristic of excited state decay or orientational redistribution.

Fig. 3.1.2 Orientation relaxation times versus solution viscosity for R-6G in different solvents (93).

Fig. 3.1.3 Structure of the triphenylmethane dye crystal violet. Symmetry is D_3 with the phenyl groups at an angle to the molecular plane giving the molecule a propeller-like conformation. The structures of other triphenylmethane dyes are similar.

Fig. 3.1.4 A) Driven rotation kinetic model requires the difference in ground and excited state potential energy minima to be large. The viscosity dependence of the ring rotation rate $K\theta$ accounts for the variation of the fluorescence quantum yield with viscosity. B) Results of ground state repopulation experiments can

be explained by considering the potential surfaces to be shallow, with the excited state surface somewhat shallower than that of the ground state. This results in excited molecules having distinct decay rates over a wide range of values. Observed viscosity dependence of kinetics results from ring rotation in low viscosity solvents.

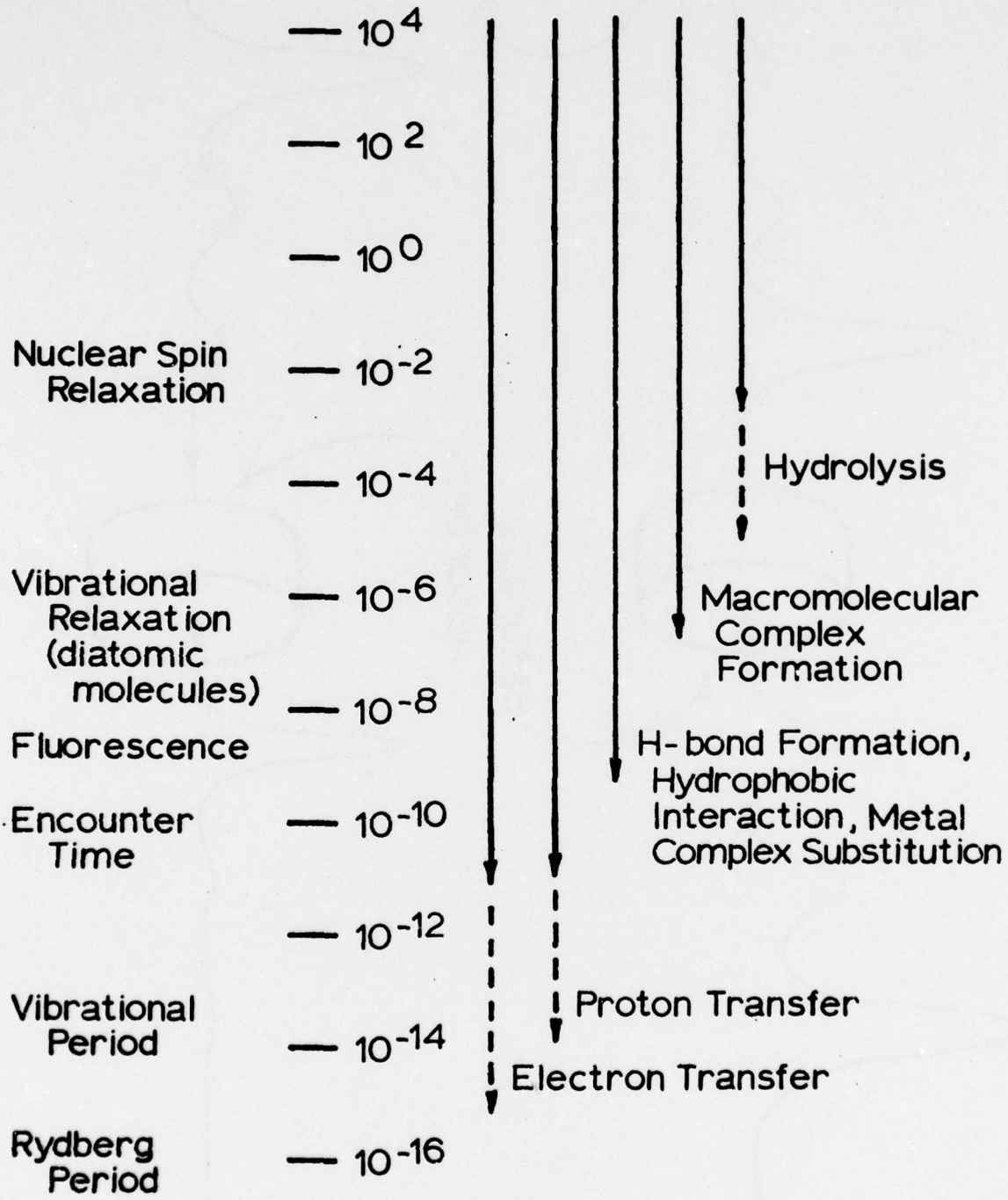
10^4
10^2
10^0
10^{-2}
10^{-4}
10^{-6}
10^{-8}
10^{-10}
10^{-12}
10^{-14}
10^{-16}
Nuclear Spin Relaxation
Vibrational Relaxation (diatomic molecules)
Fluorescence
Encounter Time
Vibrational Period
Rydberg Period
Hydrolysis
Macromolecular Complex Formation
H-bond Formation, Hydrophobic Interaction, Metal Complex Substitution
Proton Transfer
Electron Transfer

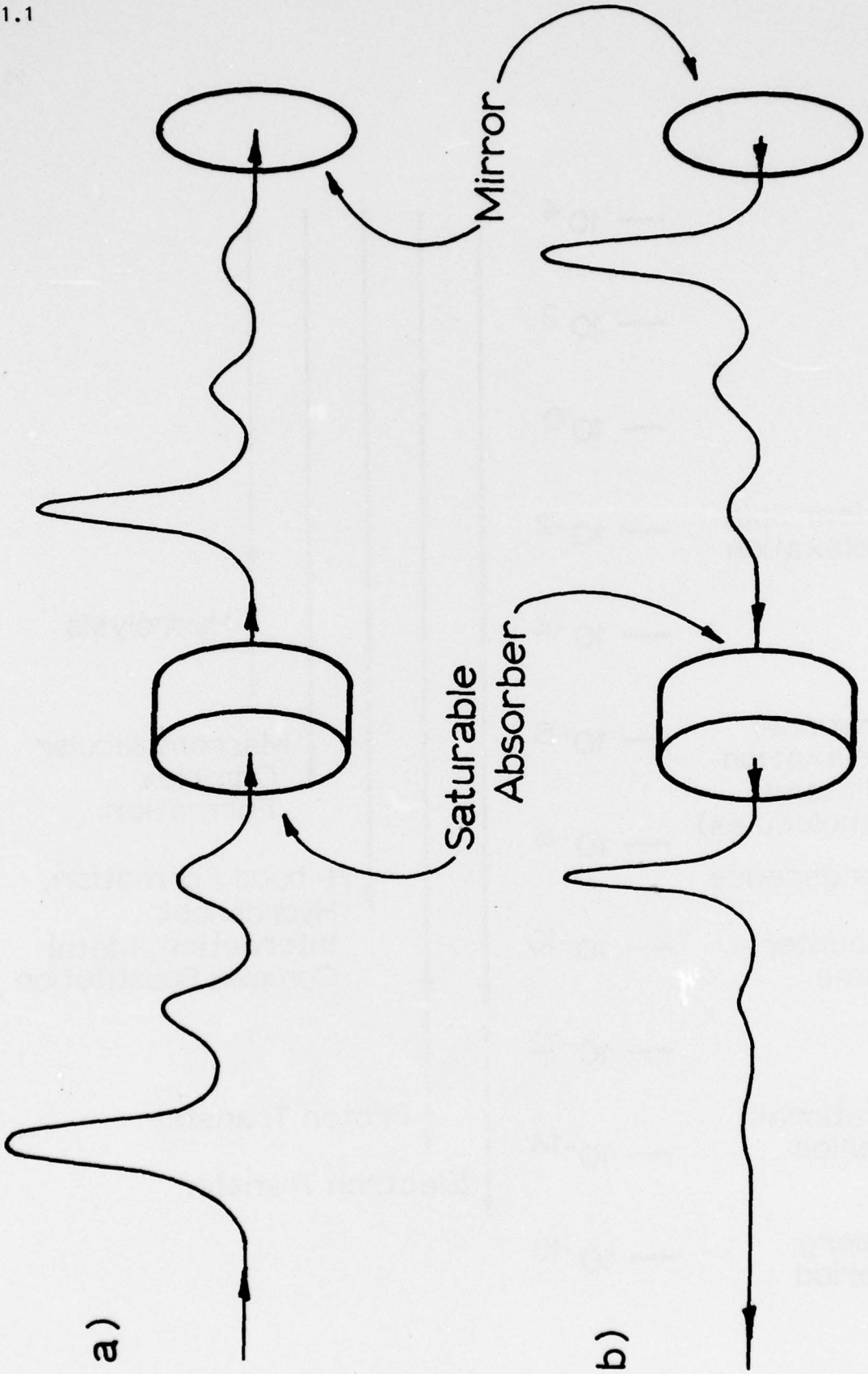
Mirror
Saturable
Absorber
a)
b)

Output Mirror
(T ~0.05)
Mode Locked
Pulse Train
Gain Medium
(jet stream)
Contact Dye
Cell (flowing dye)
~0.5 mm
f.l. = 2.5 cm
Argon Laser Input

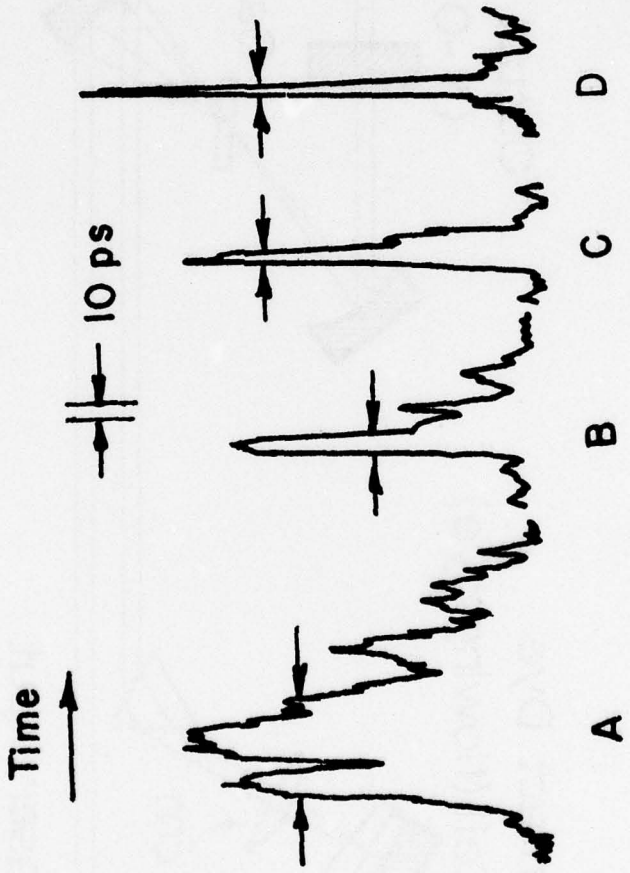
Time
10 ps
A
B
C
D

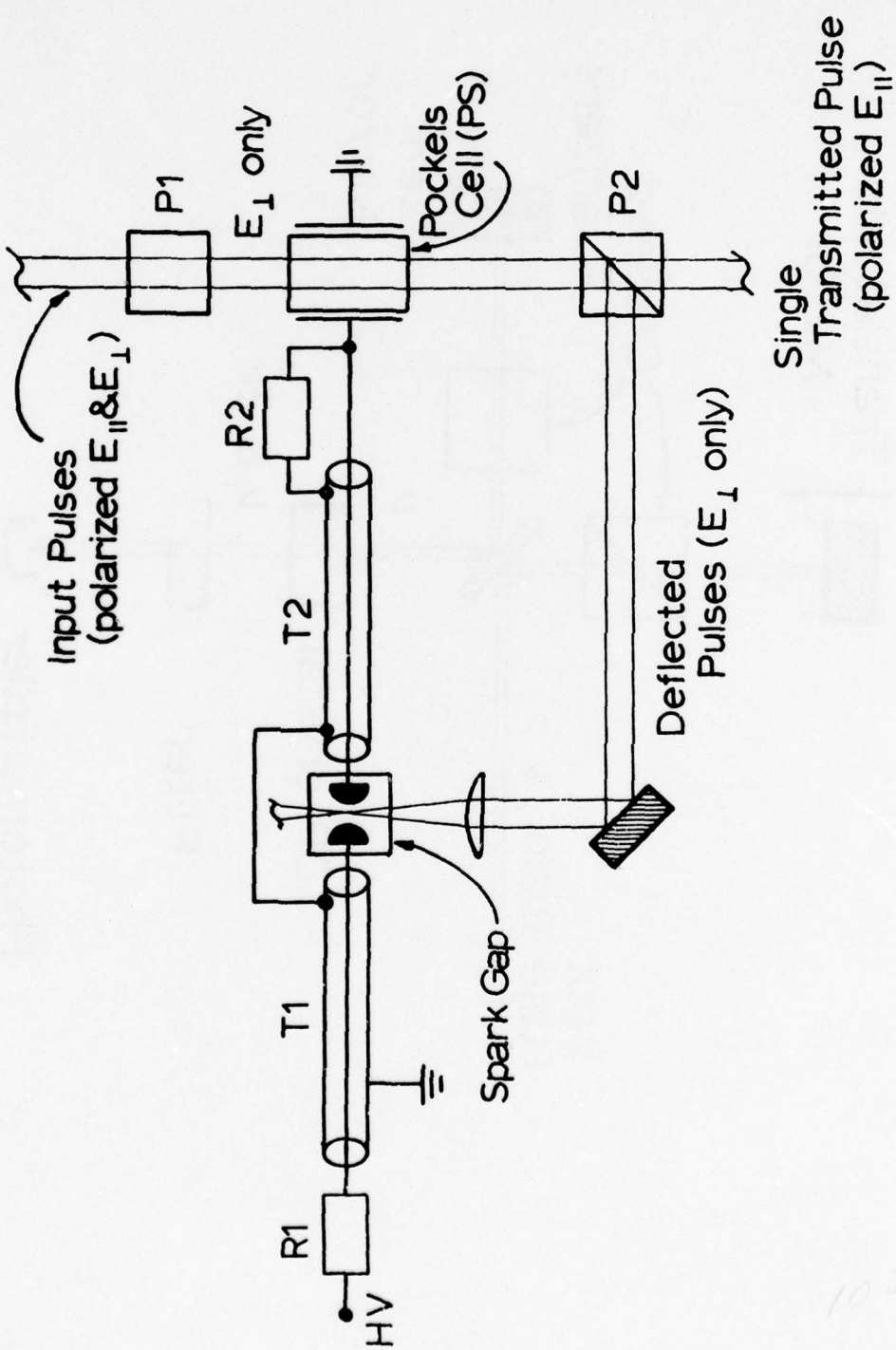
Input Pulses
(polarized $E_{\parallel}$&$E_{\perp}$)
P1
$E_{\perp}$ only
Pockels
Cell (PS)
P2
Single
Transmitted Pulse
(polarized $E_{\parallel}$)
R2
T2
Deflected
Pulses ($E_{\perp}$ only)
T1
Spark Gap
R1
HV

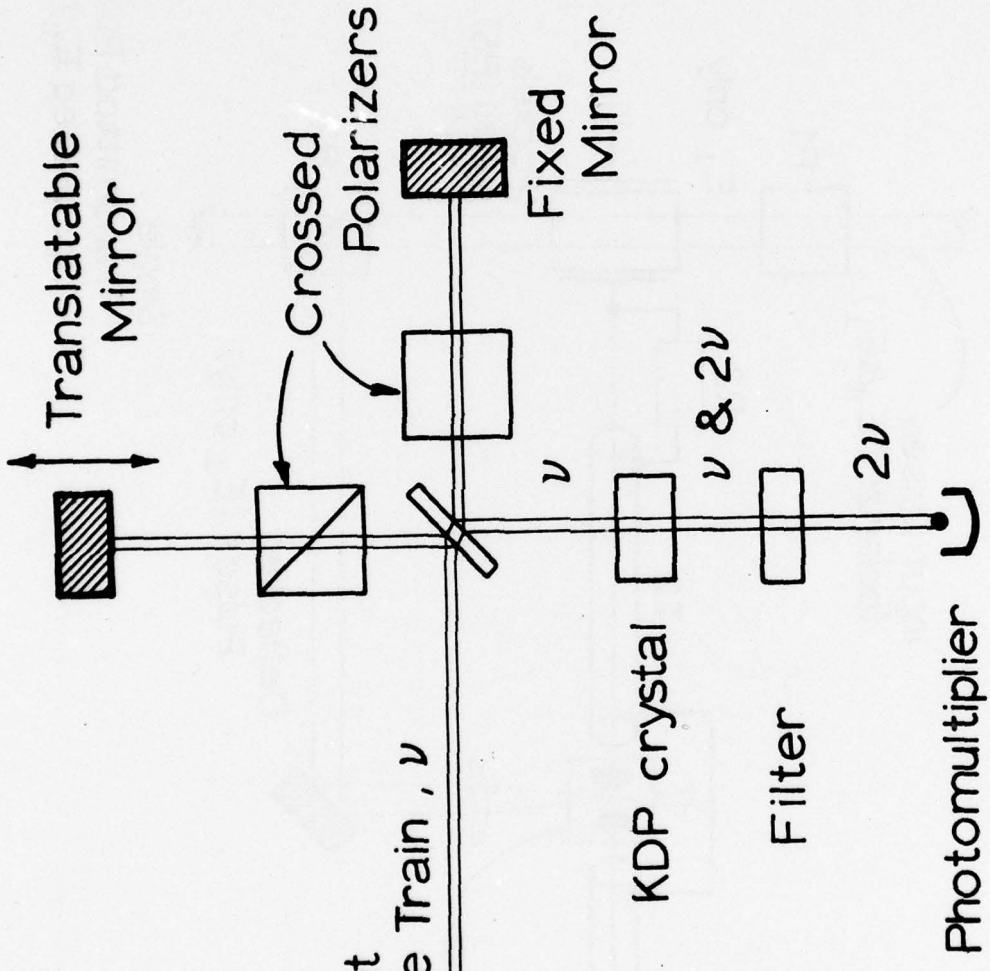
Translatable Mirror
Crossed Polarizers
Fixed Mirror
ν
ν & 2ν
2ν
Input Pulse Train , ν
KDP crystal
Filter
Photomultiplier

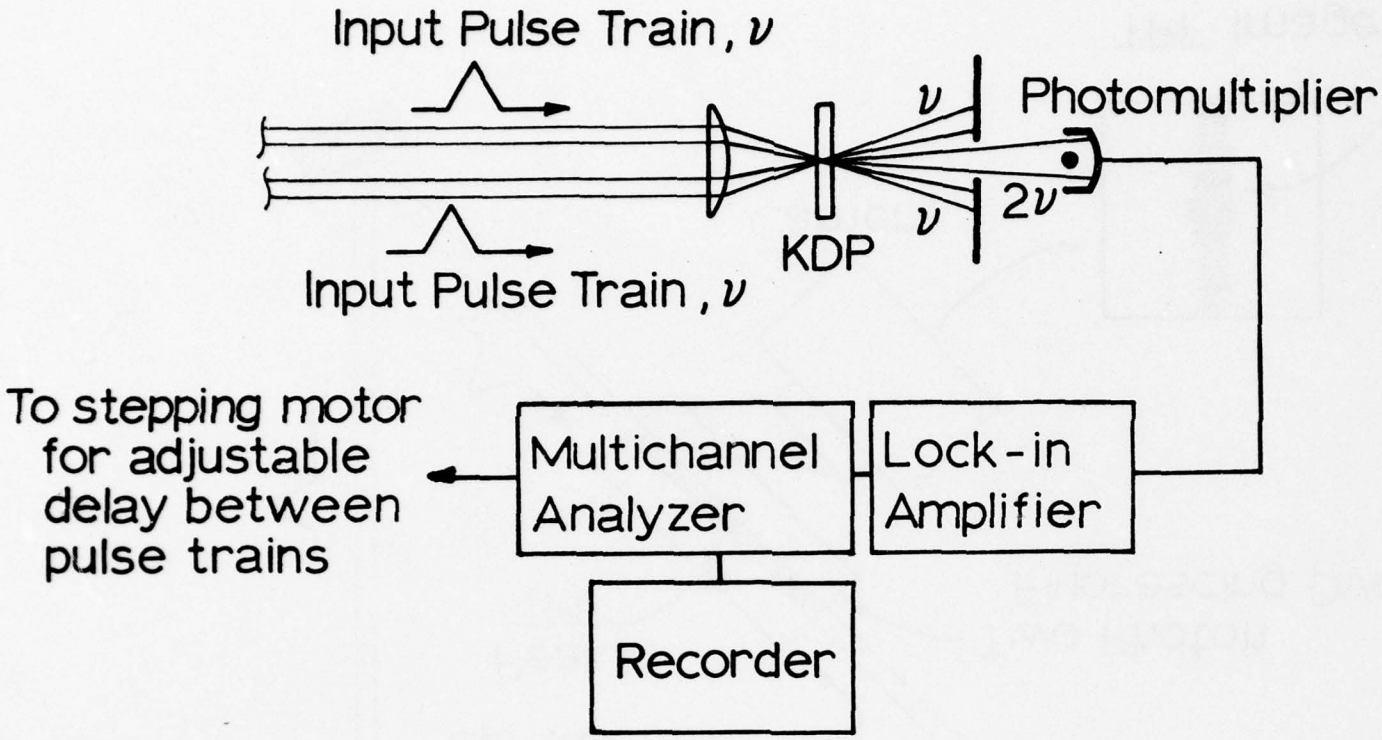
Input Pulse Train, ν
ν
Photomultiplier
2ν
ν
KDP
Input Pulse Train, ν
To stepping motor for adjustable delay between pulse trains
Multichannel Analyzer
Lock-in Amplifier
Recorder

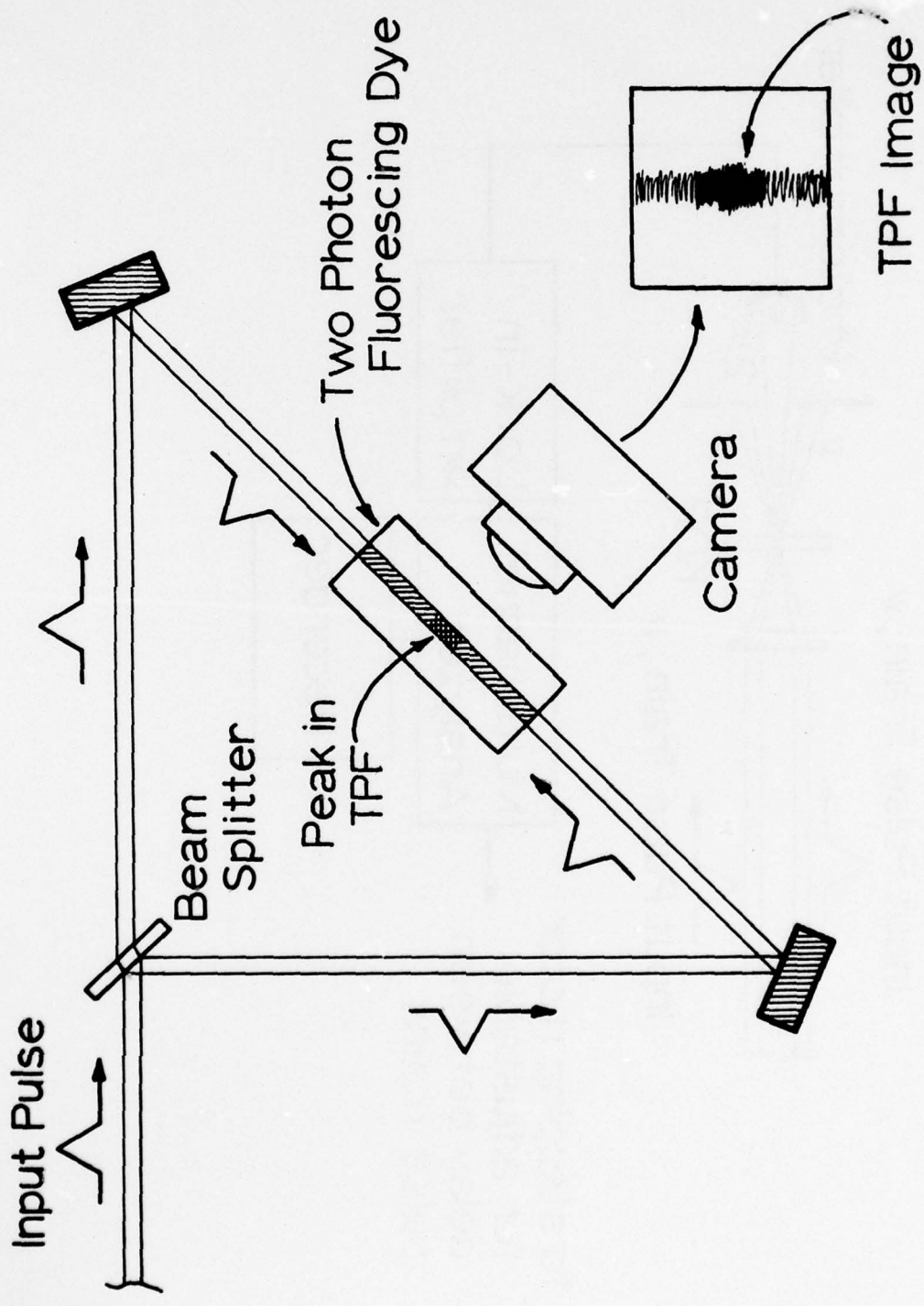
Input Pulse
Beam Splitter
Peak in TPF
Two Photon Fluorescing Dye
Camera
TPF Image

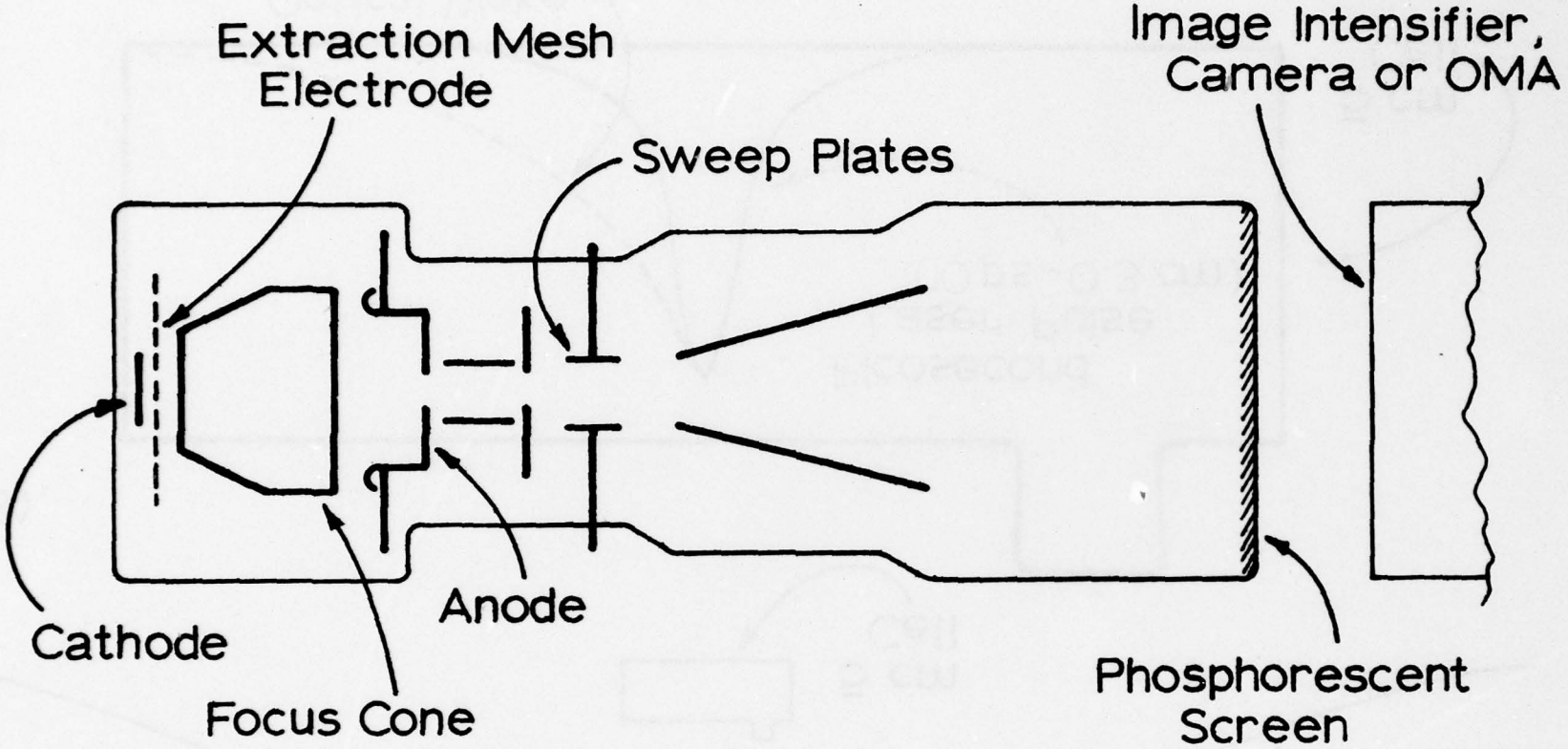
Extraction Mesh
Electrode
Sweep Plates
Image Intensifier,
Camera or OMA
Cathode
Anode
Focus Cone
Phosphorescent
Screen

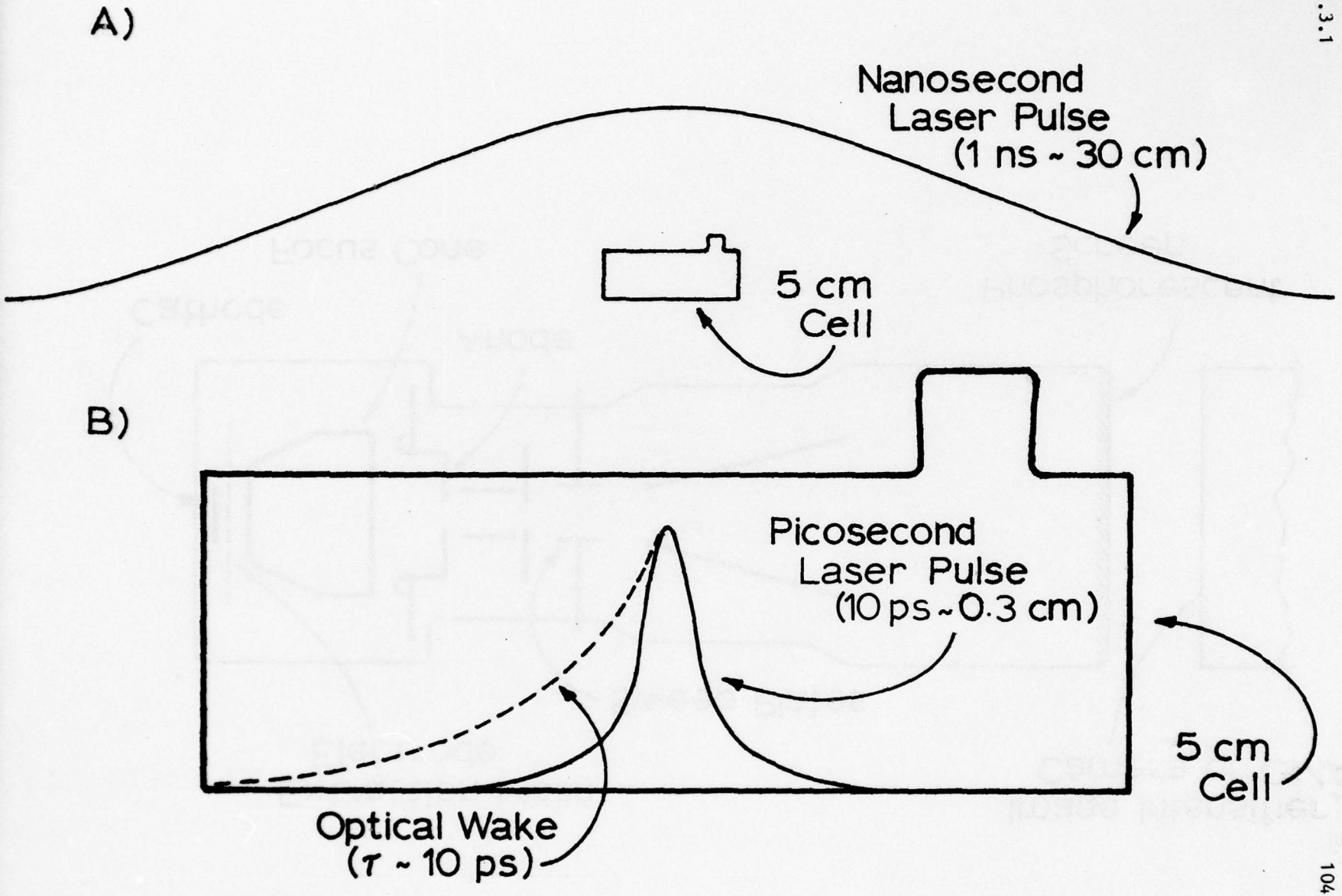
A)
Nanosecond
Laser Pulse
(1 ns ~ 30 cm)
5 cm
Cell
B)
Picosecond
Laser Pulse
(10 ps ~ 0.3 cm)
5 cm
Cell
Optical Wake
(τ ~ 10 ps)

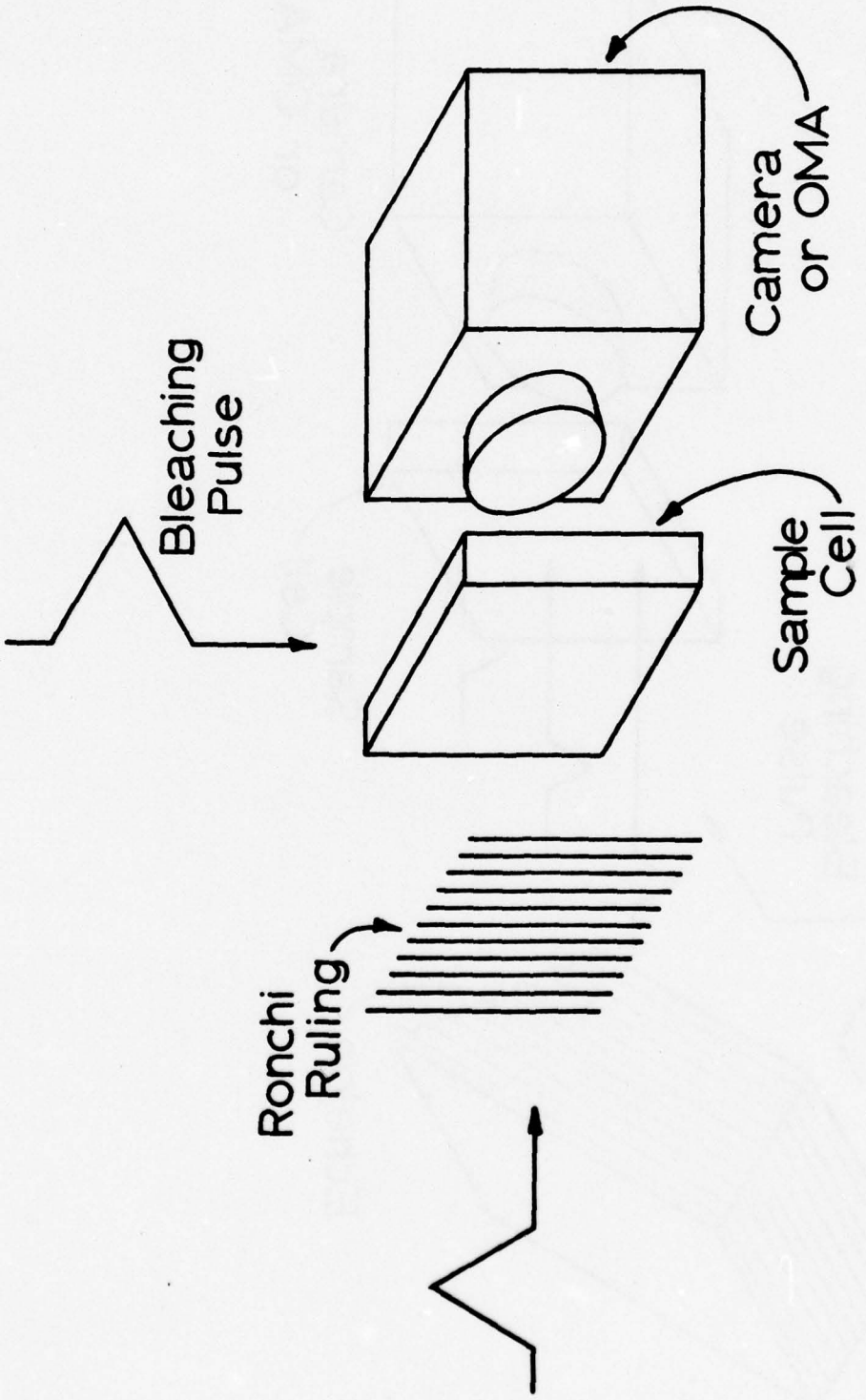
Camera
or OMA
Bleaching
Pulse
Sample
Cell
Ronchi
Ruling

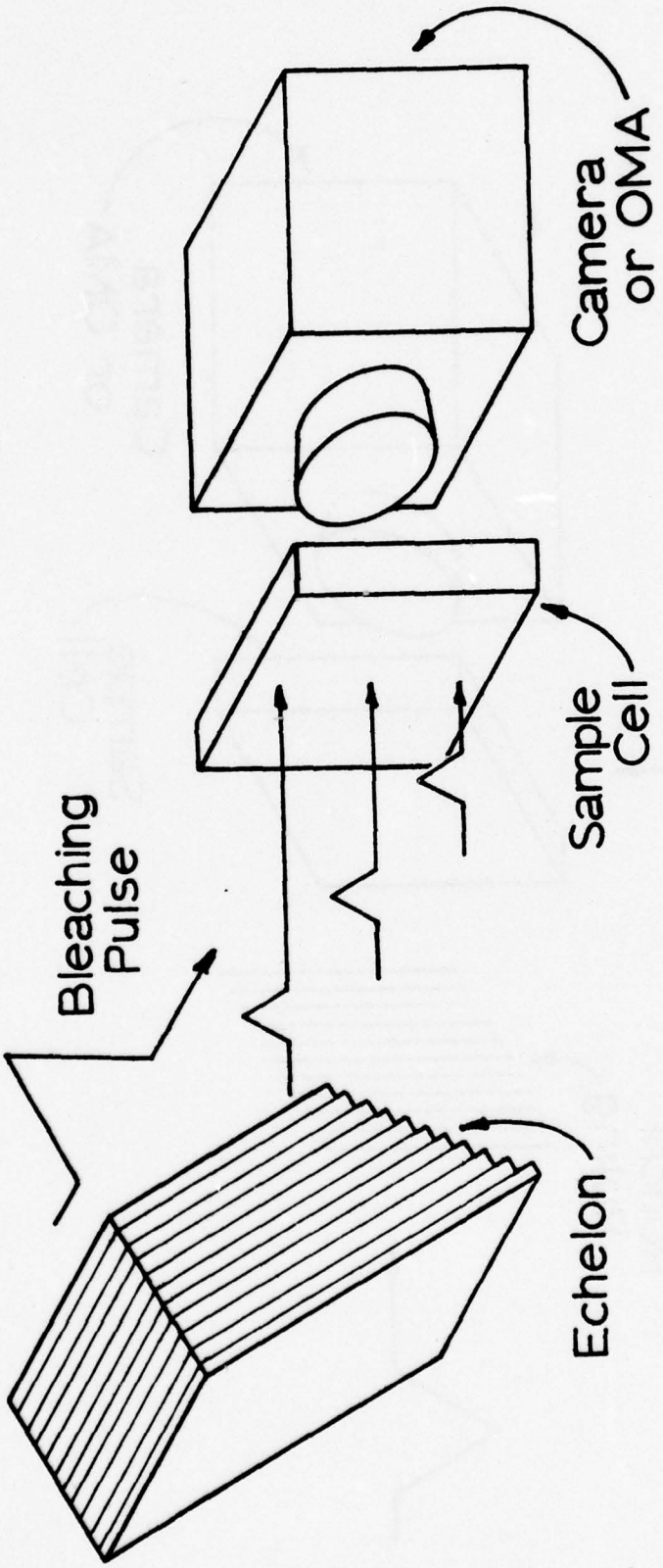
Camera
or OMA
Sample
Cell
Bleaching
Pulse
Echelon

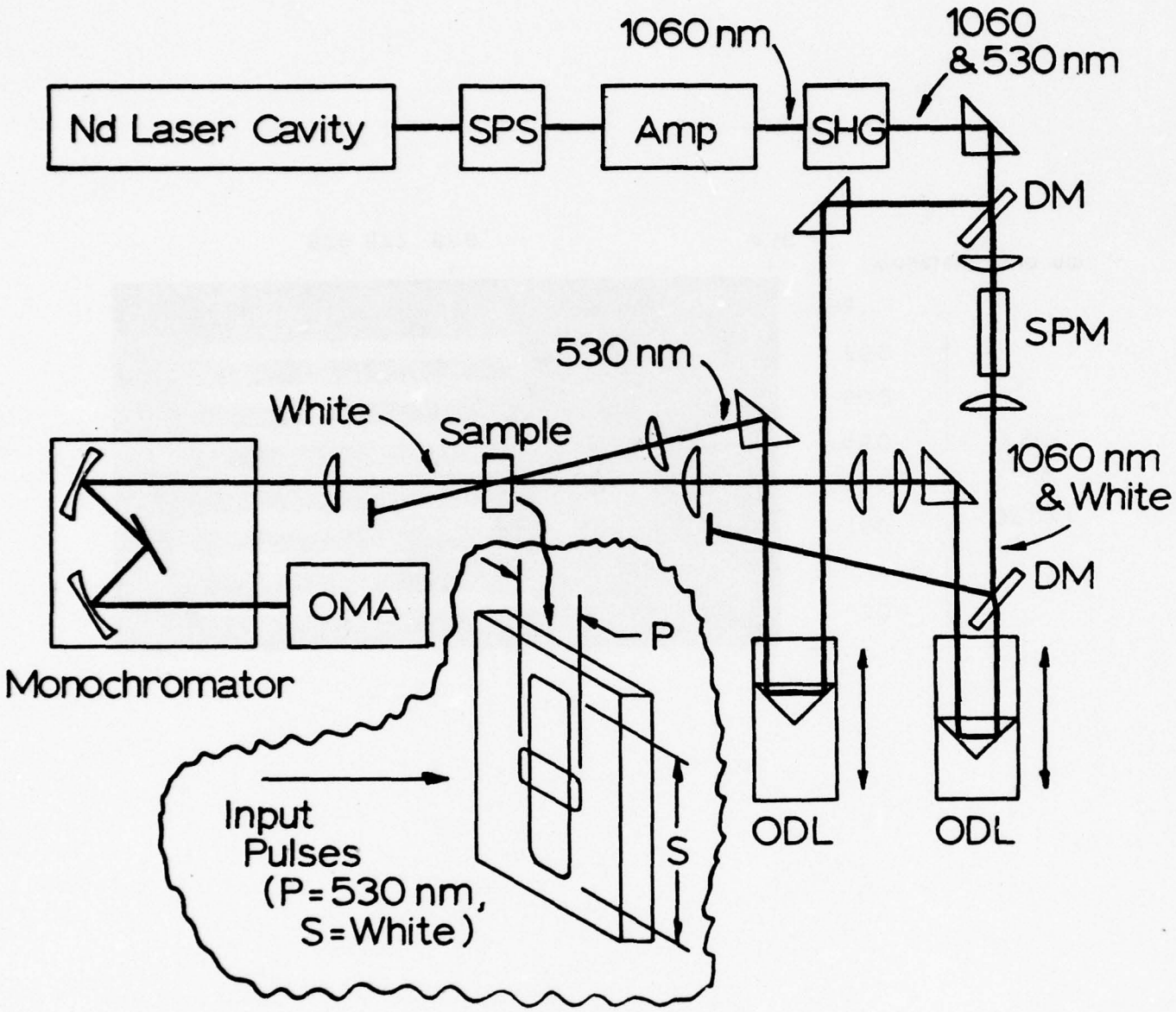
1060 nm
1060
& 530 nm
Nd Laser Cavity
SPS
Amp
SHG
DM
SPM
530 nm
White
Sample
1060 nm
& White
DM
OMA
Monochromator
P
S
Input
Pulses
(P=530 nm,
S=White)
ODL
ODL

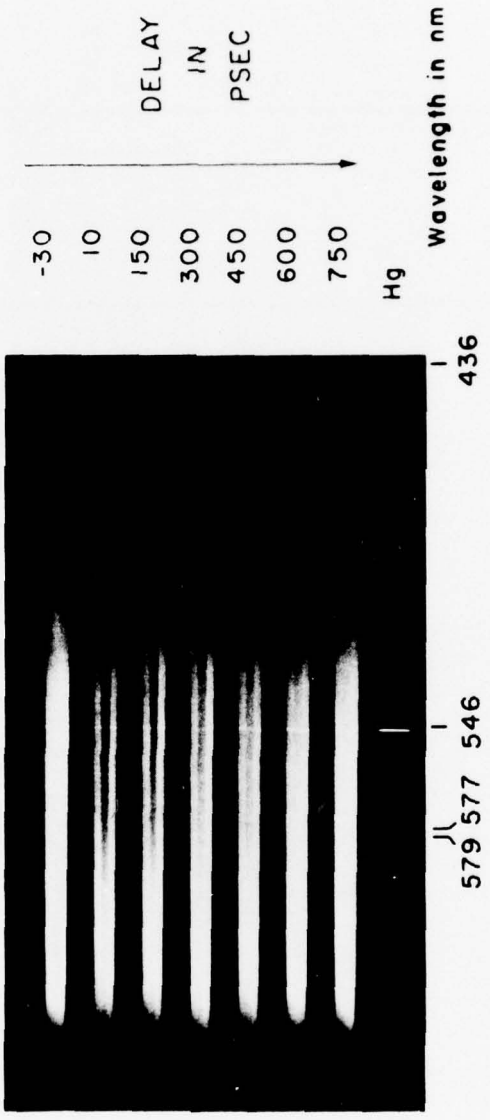
-30
10
150
300
450
600
750
DELAY
IN
PSEC
Hg
Wavelength in nm
436
546
579 577

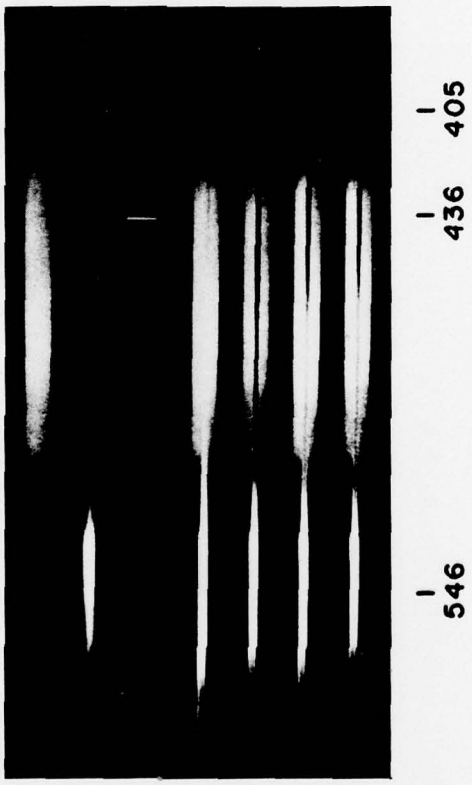
S only
P + Sn Cℓ2 OEP
Hg
-20
+40
500
2000
P+S DELAY IN PSEC
Hg Wavelength
546
436
405

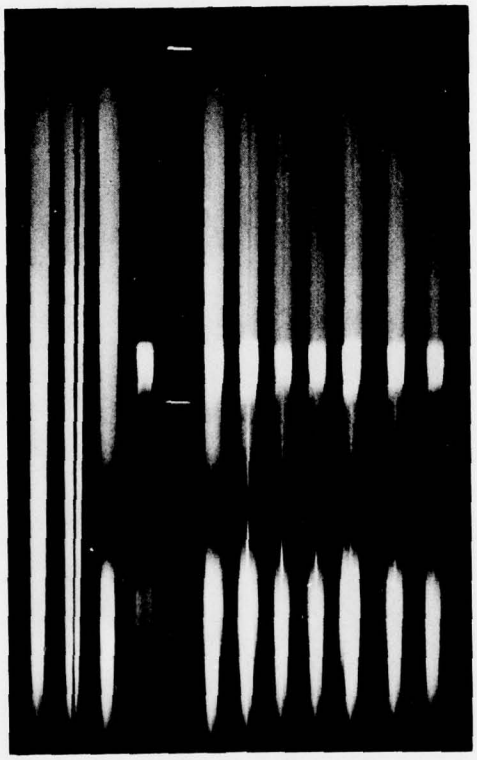
S only
S + opaque absorber
S + DODCI
P only
Hg
-20
+20
300
600
900
1500
2400
P+S DELAY IN PSEC
Hg Wavelength in nm
436
546
577
579

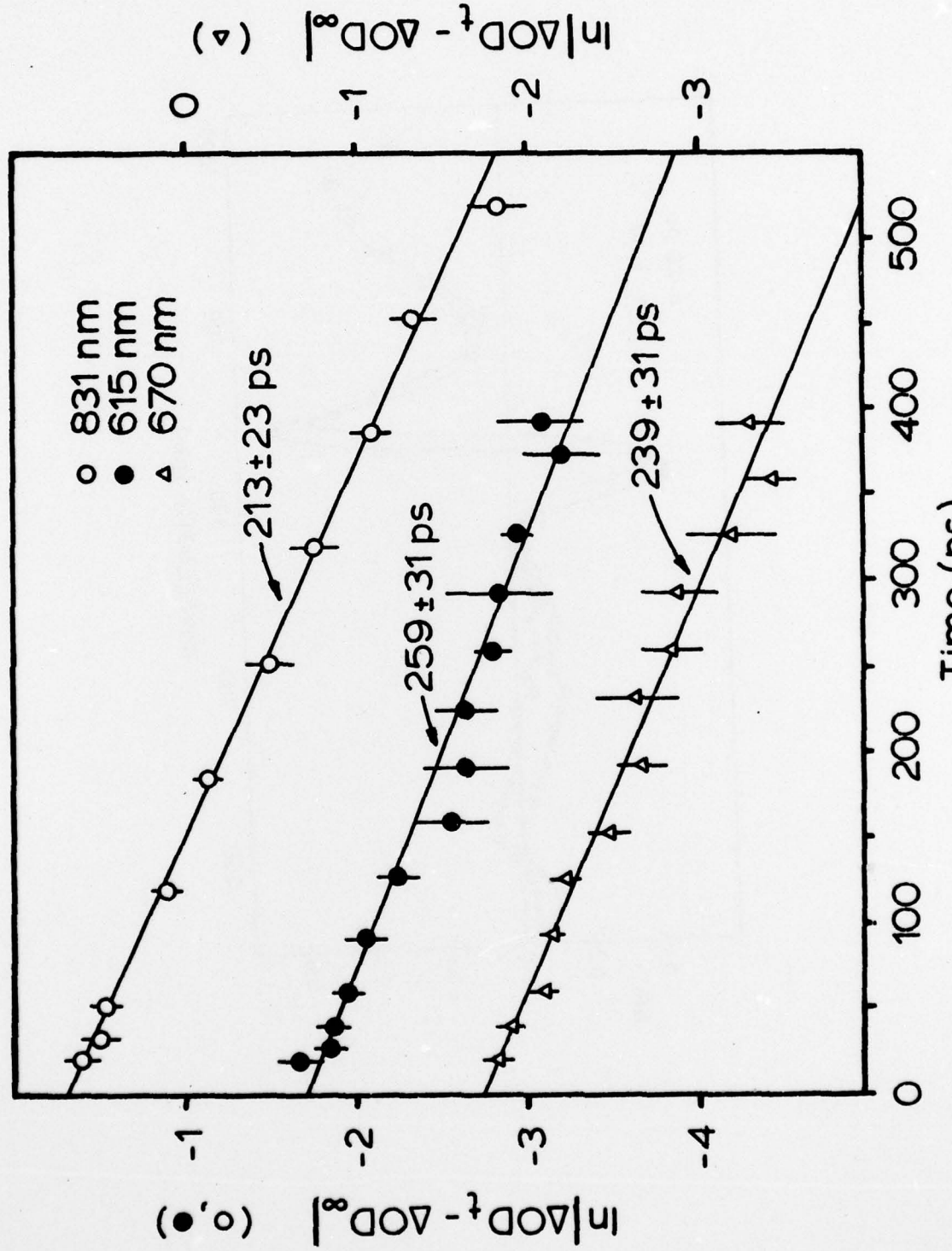
ln|ΔOD_t - ΔOD_∞| (o,●)
ln|ΔOD_t - ΔOD_∞| (▲)
831 nm
615 nm
670 nm
213±23 ps
259±31 ps
239±31 ps
Time (ps)
0
100
200
300
400
500
-1
-2
-3
-4

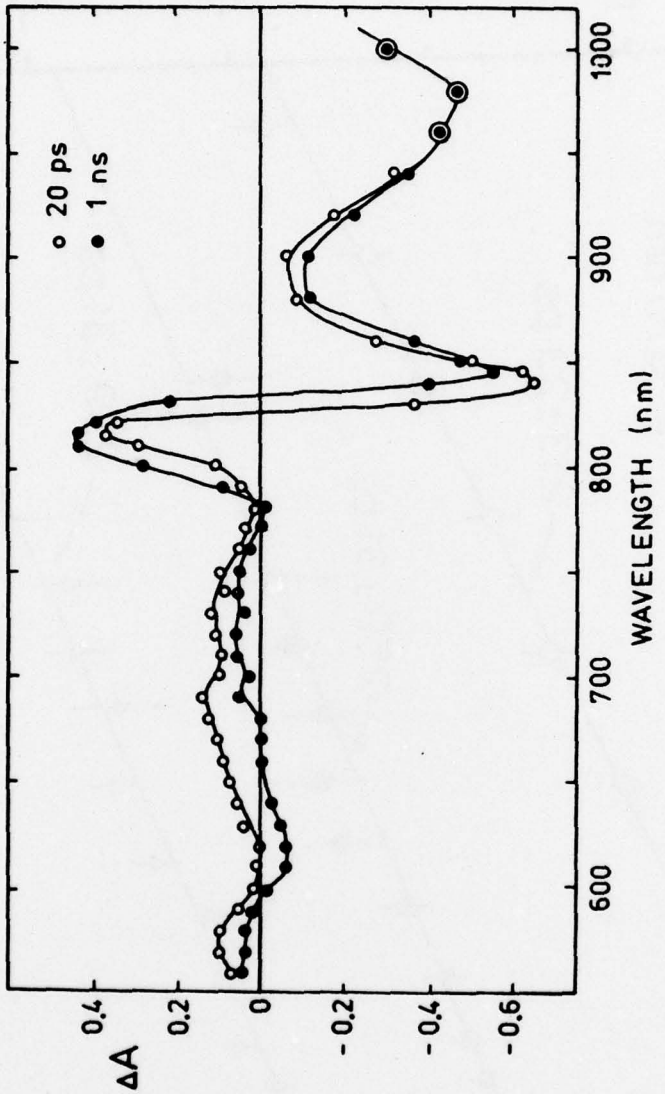
o 20 ps
• 1 ns
ΔA
0.4
0.2
0
-0.2
-0.4
-0.6
600
700
800
900
1000
WAVELENGTH (nm)

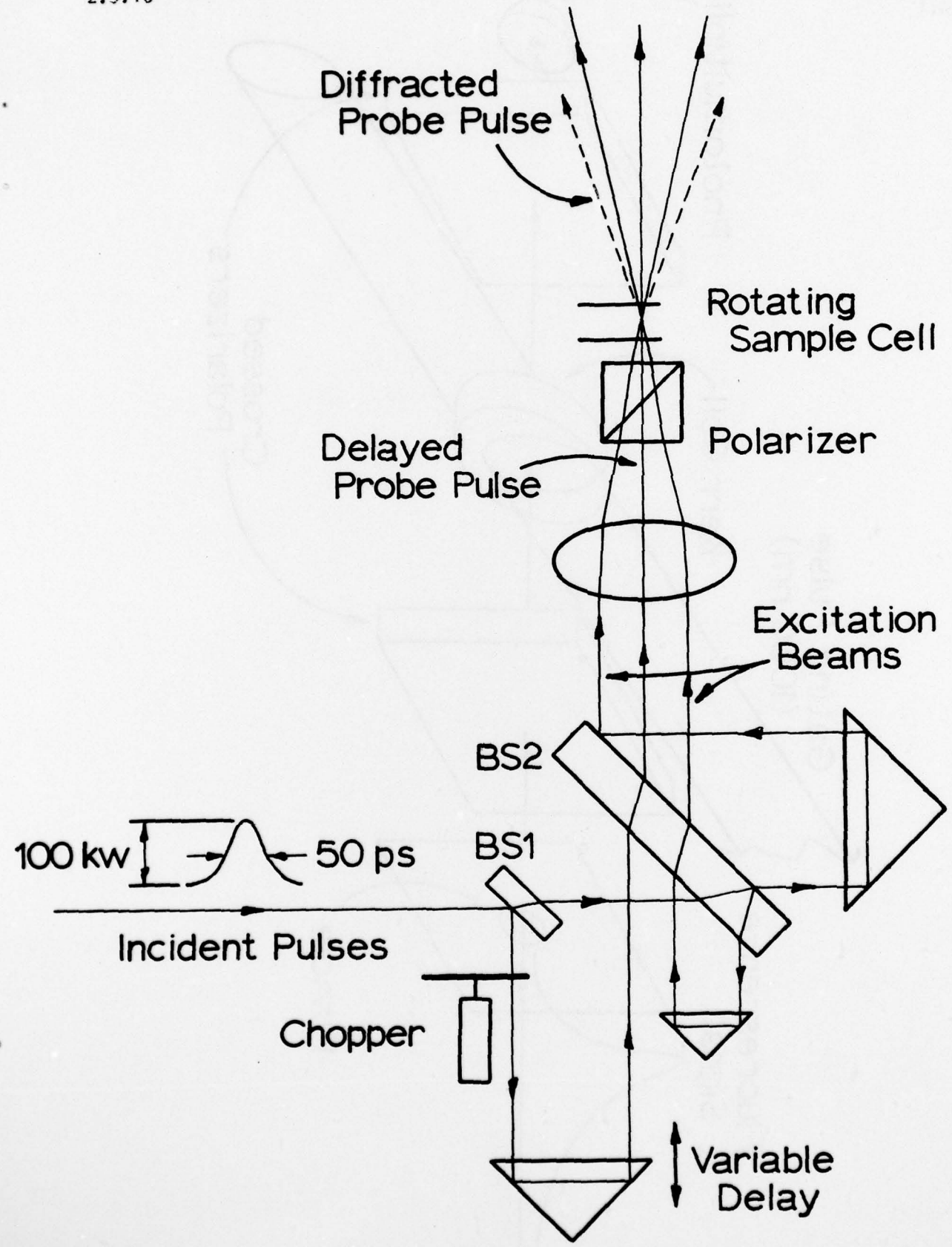
Diffracted
Probe Pulse
Rotating
Sample Cell
Polarizer
Delayed
Probe Pulse
Excitation
Beams
BS2
100 kw
50 ps
BS1
Incident Pulses
Chopper
Variable
Delay

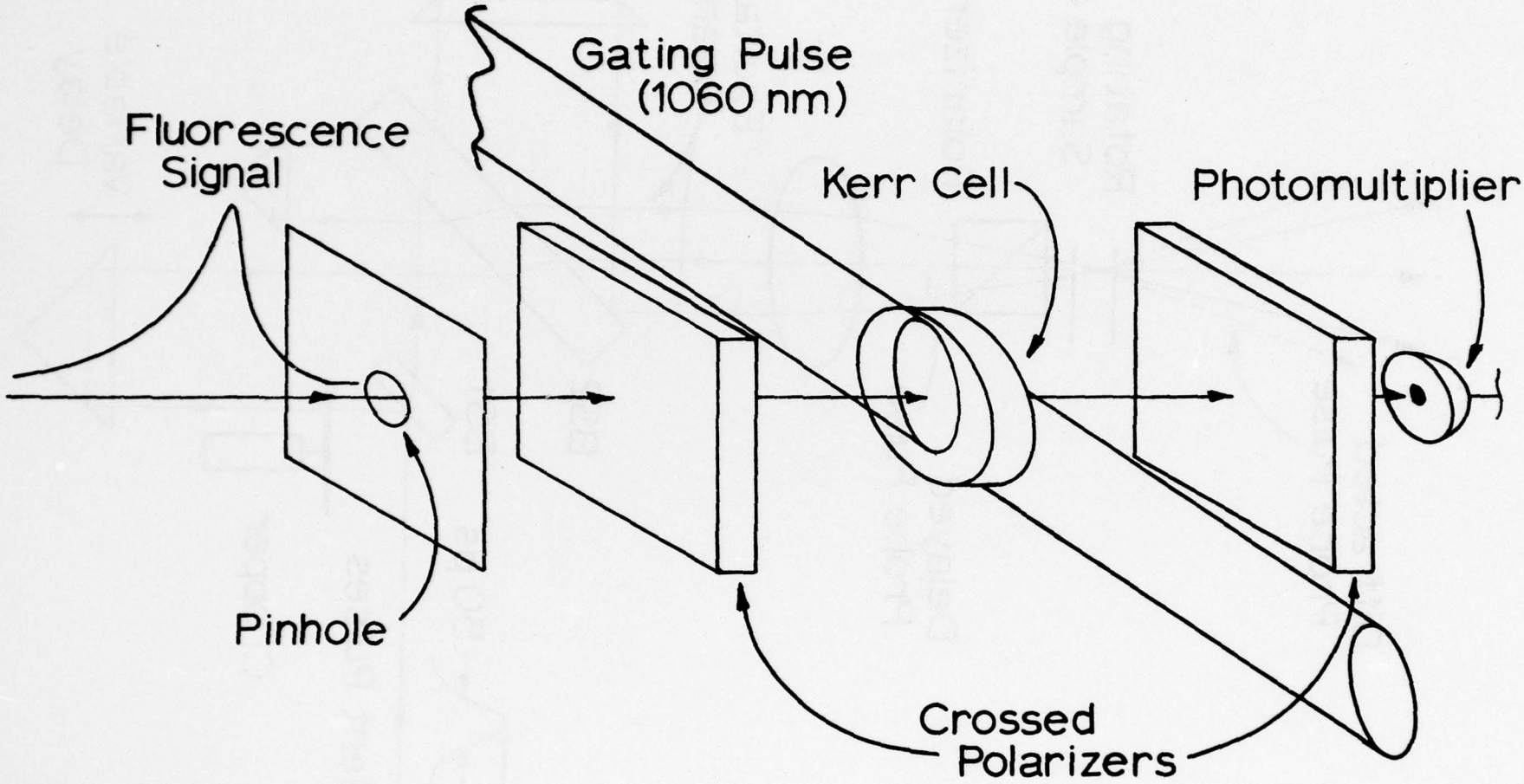
Gating Pulse
(1060 nm)
Fluorescence
Signal
Kerr Cell
Photomultiplier
Pinhole
Crossed
Polarizers

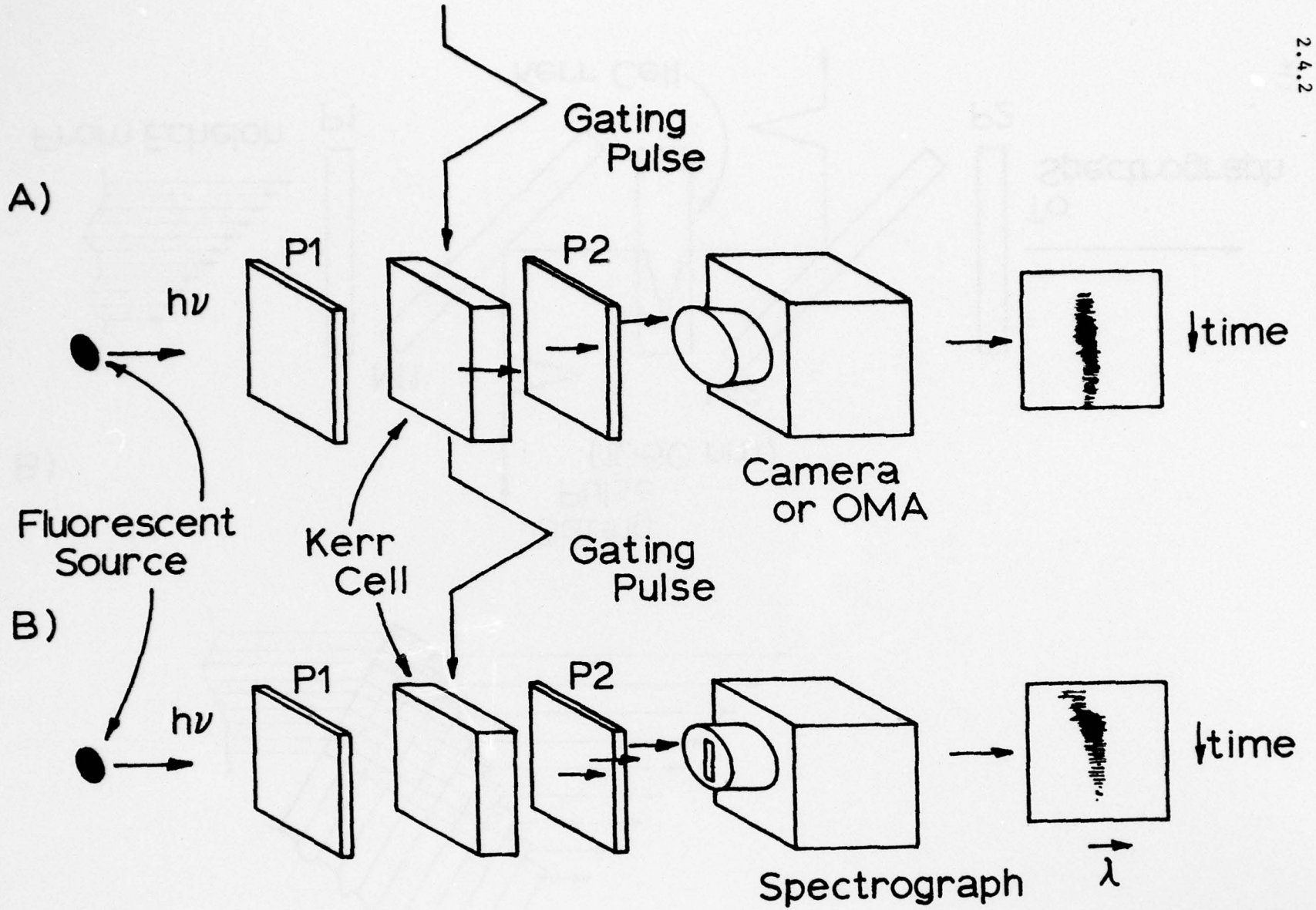
A)
Gating
Pulse
P1
P2
hν
time
Camera
or OMA
Fluorescent
Source
Kerr
Cell
Gating
Pulse
B)
P1
P2
hν
time
Spectrograph
λ

A)

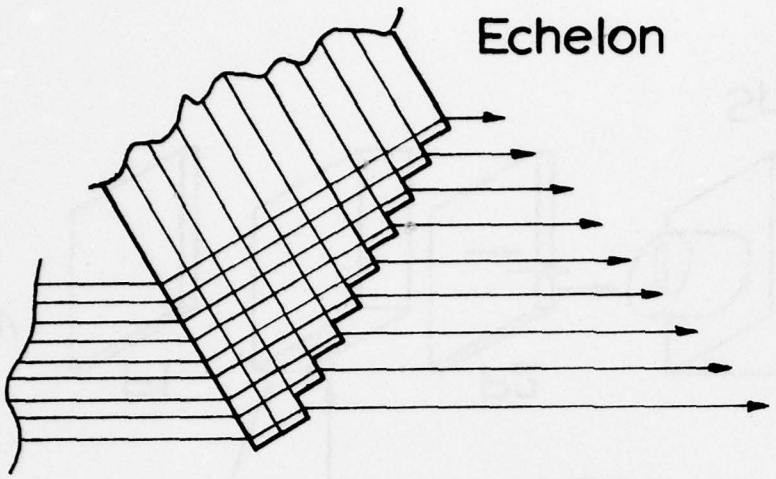
Echelon

B)

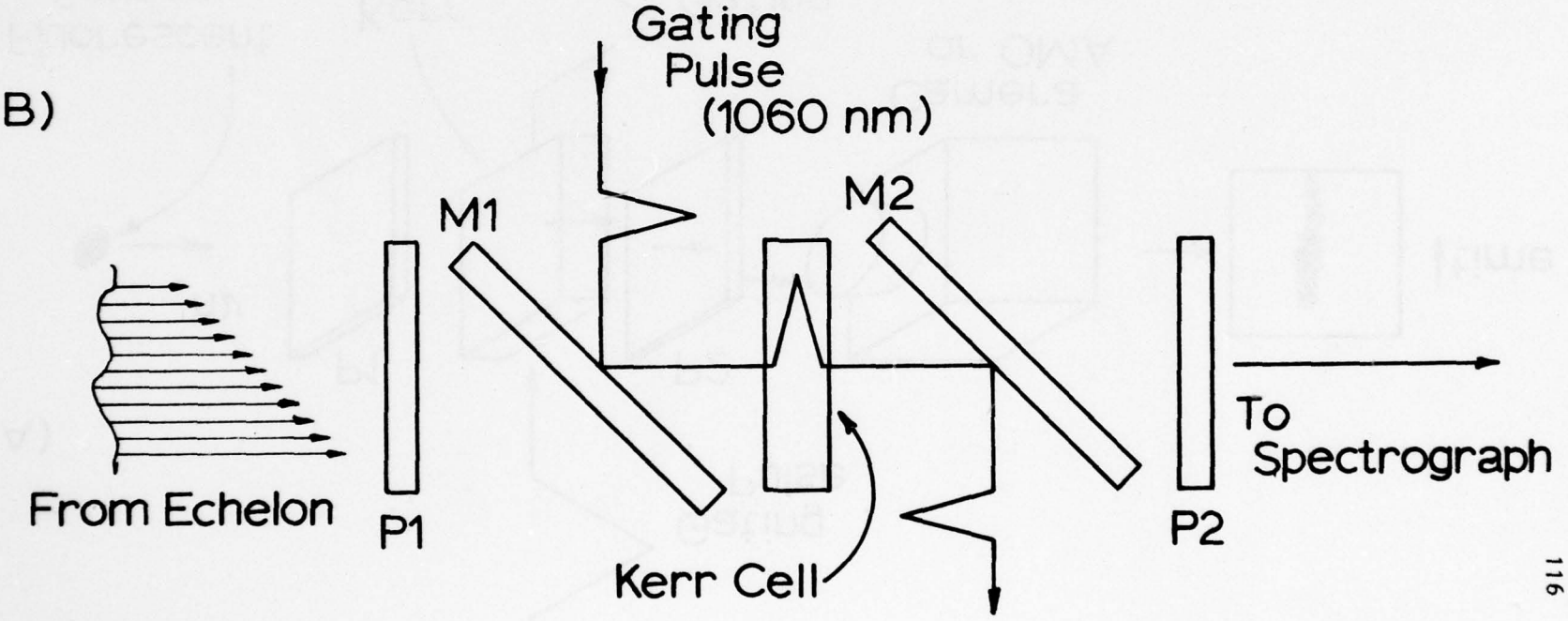
Gating
Pulse
(1060 nm)
M1
M2
From Echelon
P1
Kerr Cell
P2
To
Spectrograph

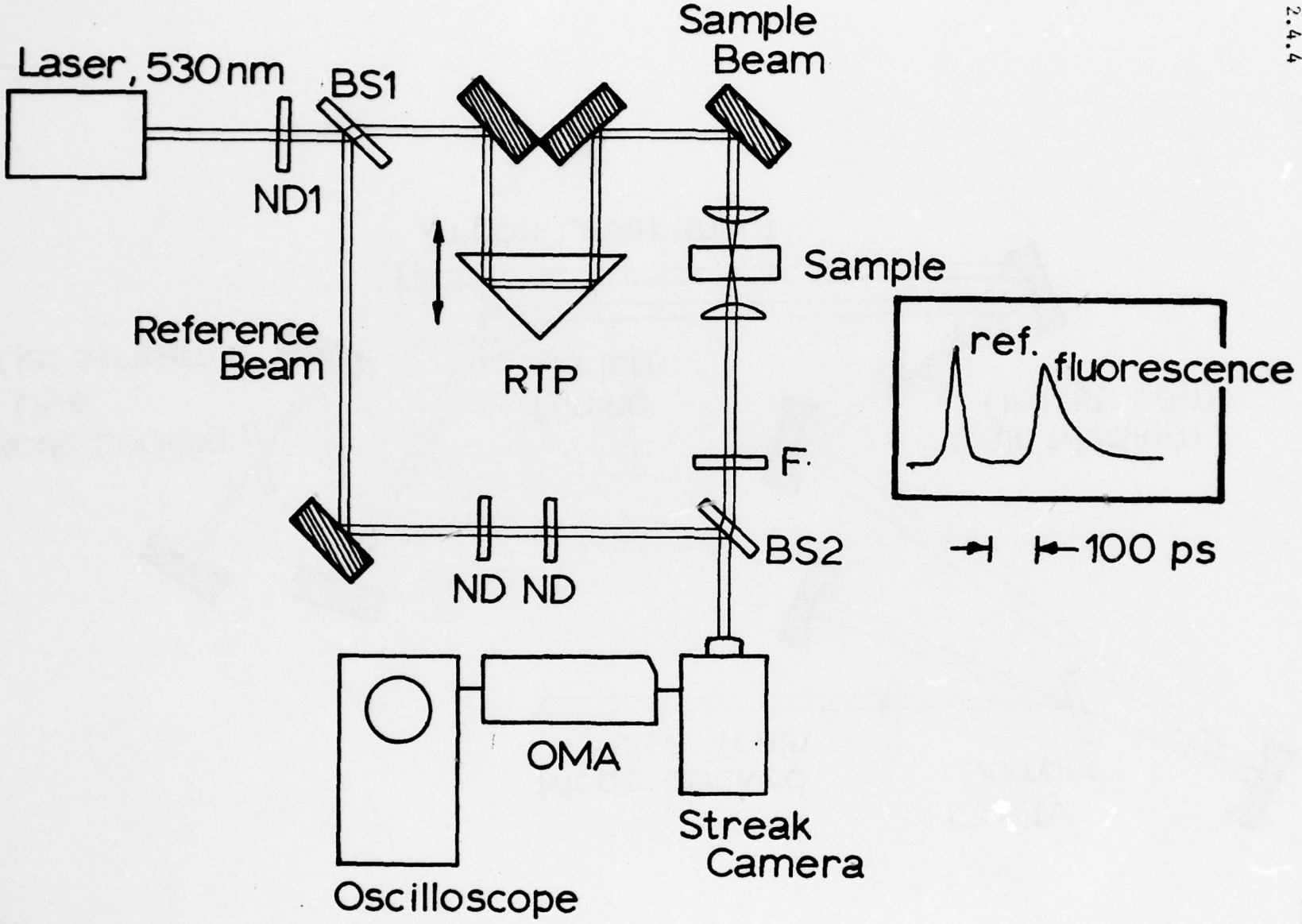
Laser, 530 nm
BS1
ND1
Sample Beam
Sample
Reference Beam
RTP
F
BS2
ND ND
OMA
Streak Camera
Oscilloscope
ref.
fluorescence
100 ps

Cavity
Dumper
Gain Medium
(jet stream)
Mode Locked
Pulse Train
Tuning
Prism
Argon Laser Input
Mode Locking
Dye
(jet stream)

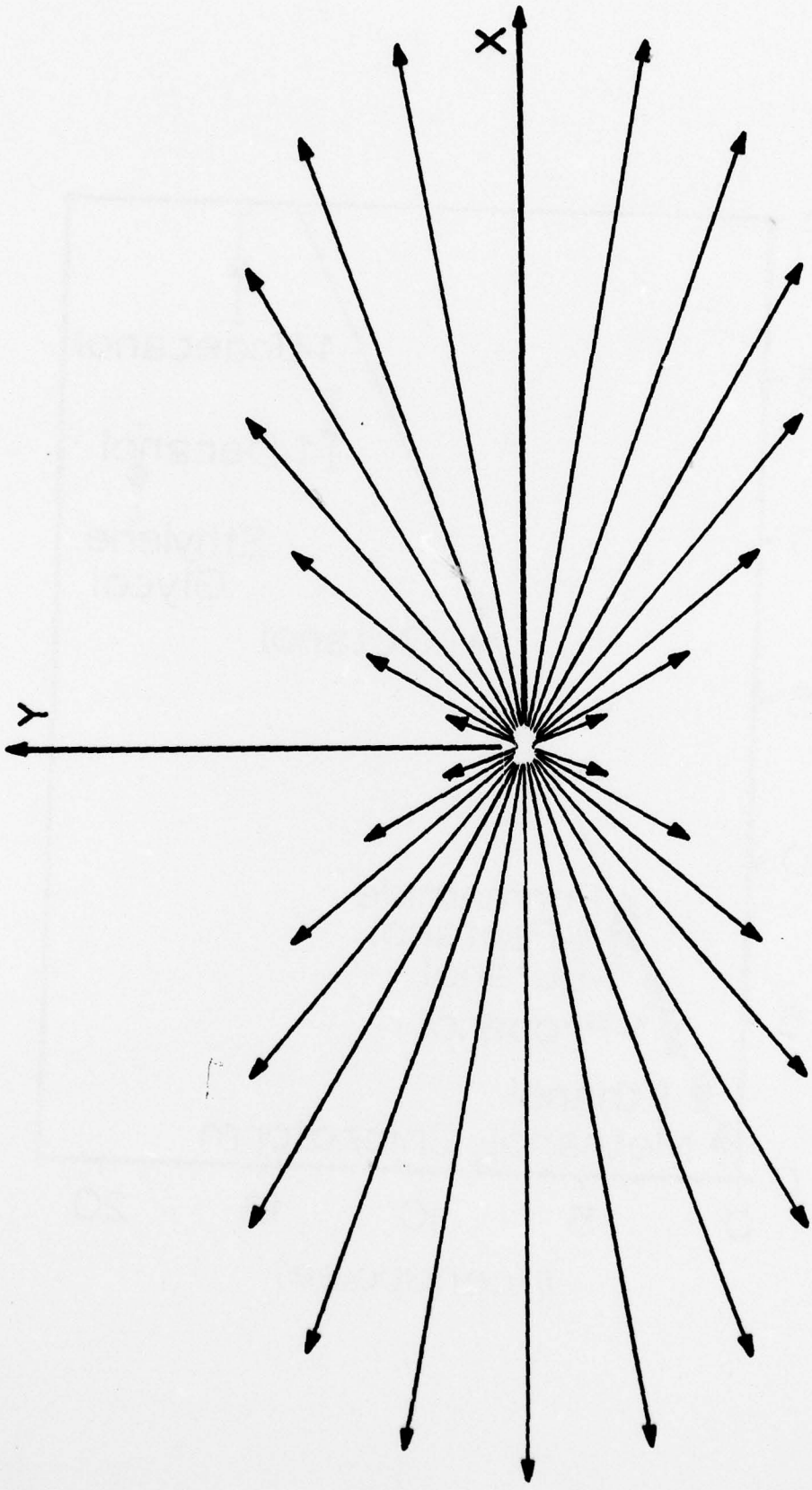
X
Y

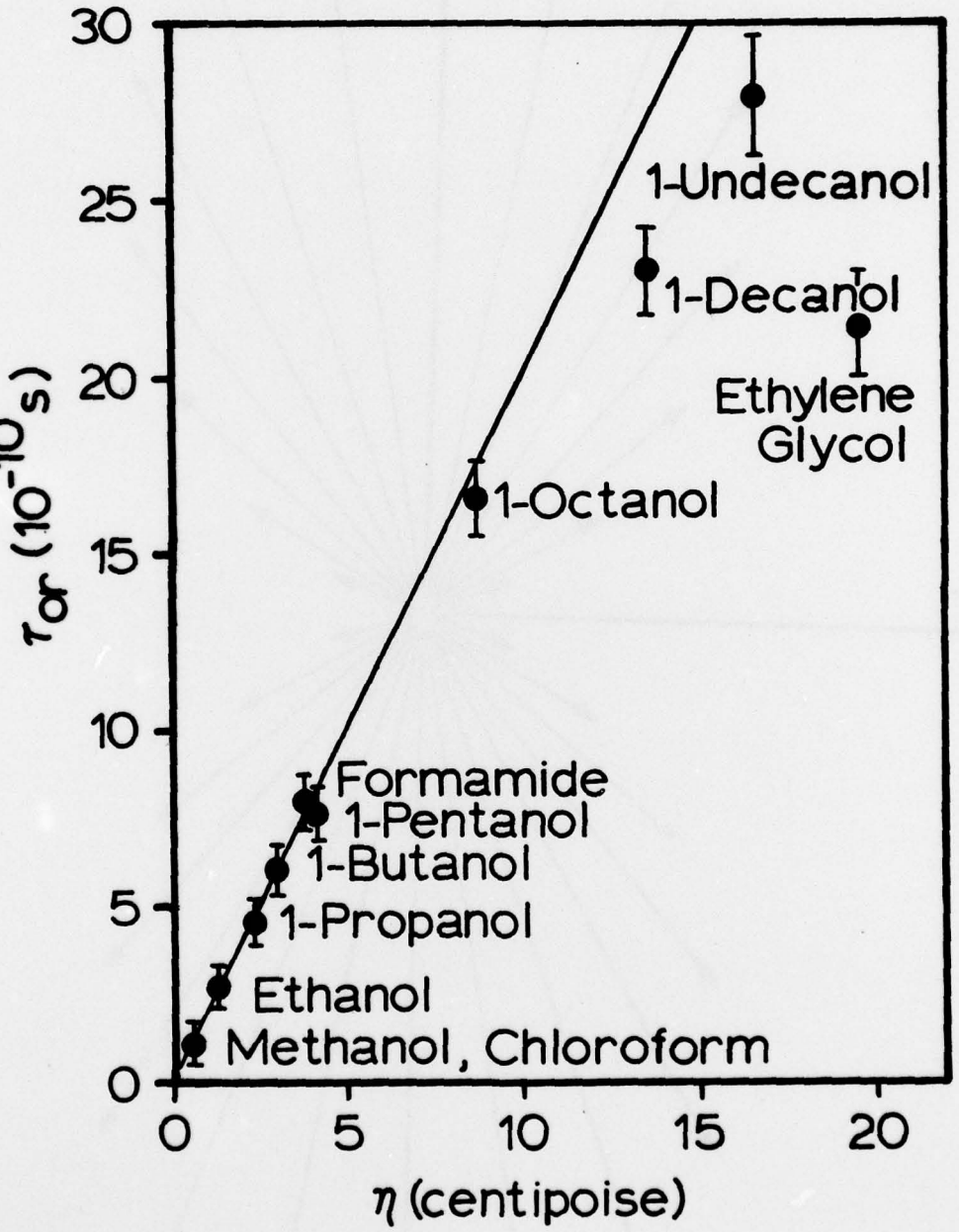
30
25
20
15
10
5
0
τ_{or} (10^{-10} s)
0
5
10
15
20
η (centipoise)
1-Undecanol
1-Decanol
Ethylene Glycol
1-Octanol
Formamide
1-Pentanol
1-Butanol
1-Propanol
Ethanol
Methanol, Chloroform

+
N(CH3)2
N(CH3)2
(CH3)2N

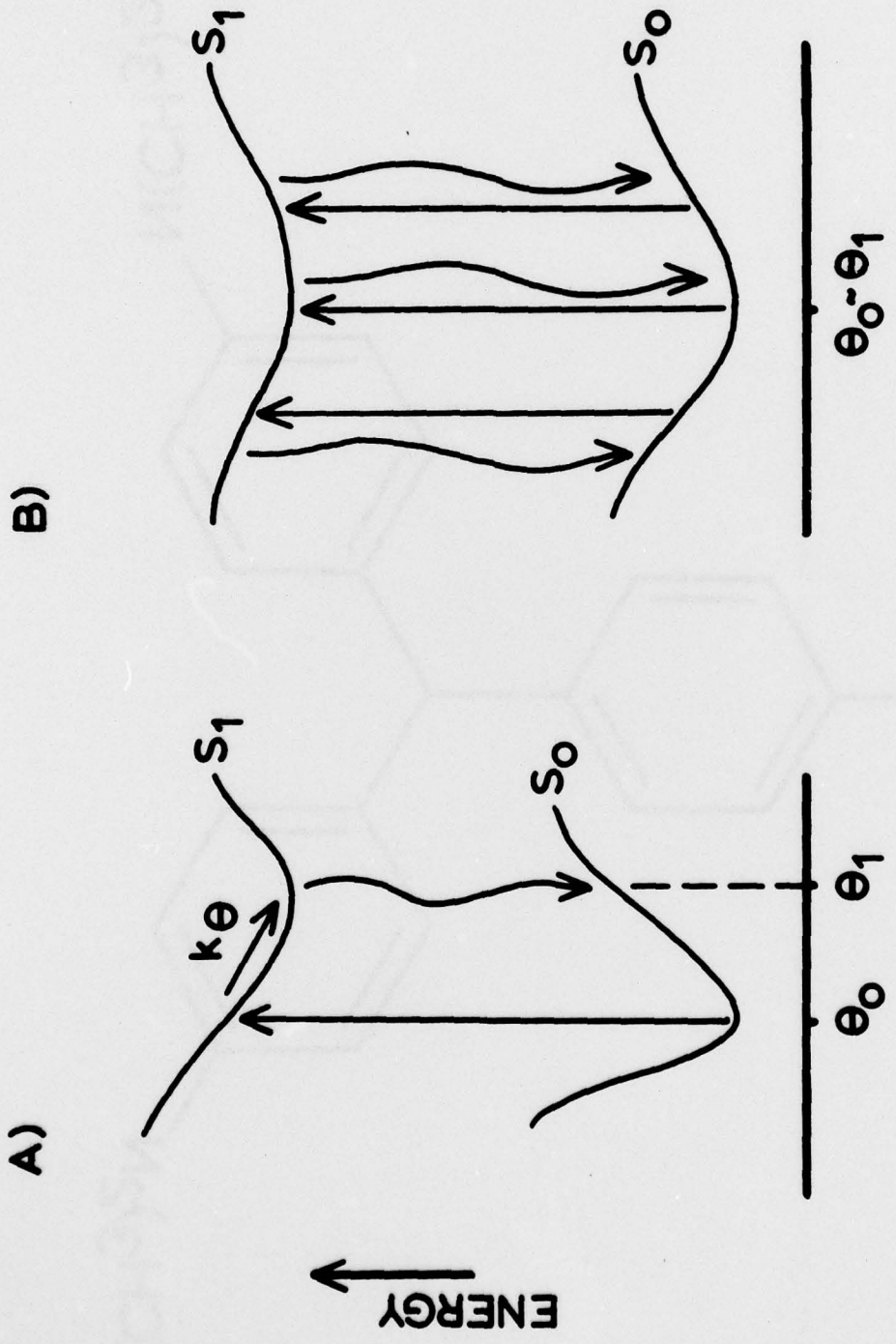
B)
S_1
S_0
θ_0-θ_1
A)
S_1
S_0
$k\theta$
θ_1
θ_0
ENERGY